

Strengthening of Concrete Structures using Steel Wire Reinforced Polymer

by W. Figeys, L. Schueremans, K. Brosens,
and D. Van Gemert

Synopsis: This paper deals with a new material for external reinforcement: Steel Wire Reinforced Polymer (SWRP). It consists of thin high-strength steel fibres embedded in a polymer laminate. This innovative material combines the advantages of steel plates and CFRP, which are already used today. The material cost of SWRP is relatively low, and the laminate is quite flexible. In the feasibility part, the practical use of SWRP is studied. Further, the available design model for externally bonded reinforcement for concrete elements is confronted with the results of an experimental program, carried out at the Reyntjens Laboratory of KULeuven. The model is adapted accordingly.

Keywords: design model; external reinforcement; steel wire reinforced polymer (SWRP)

744 Figeys et al.

Wine Figeys, ir., obtained Master of Science in Architectural Engineering in 2004. She is PhD researcher at the Building Materials Division at the KULeuven. Her research topic concerns structural restoration techniques, focusing on epoxy bonded external reinforcement. She has a research grant of the Institute for the Promotion of Innovation through Science and Technology in Flanders (IWT-Vlaanderen).

Luc Schueremans, dr. ir., graduated as a civil engineer at the KULeuven in 1995. He defended his Ph. D. thesis at the end of 2001. Since 2002, he is a post-doctoral researcher at the Building Materials Division of KULeuven, Belgium. His research focuses on structural behavior of masonry, material modeling, and reliability based design and safety assessment of existing structures.

Kris Brosens, dr. ir., obtained his PhD at the Department of Civil Engineering, K.U.Leuven, Belgium in 2001. His research concerned the strengthening of concrete structures with externally bonded steel plates and fibre reinforced materials. Nowadays he works as a project engineer for Triconsult N.V., a spin-off company of the K.U.Leuven, specialized in the structural restoration of historical monuments.

Dionys Van Gemert, dr. ir., is professor of building materials science and renovation of constructions at the Department of Civil Engineering of KULeuven, Belgium. He is head of the Reyntjens Laboratory for Materials Testing. His research concerns repairing and strengthening of constructions, deterioration and protection of building materials, and concrete polymer composites.

1. INTRODUCTION

The capacity of a structure can be enhanced using the technique of externally bonded reinforcement. By adding extra reinforcement the flexural capacity, the flexural stiffness and the shear capacity are influenced. Today, mostly steel plates and carbon fibre reinforced polymer (CFRP) sheets and laminates are used. Since both materials have their own properties, they also have their preferable applications [1; 2]. Steel plates have a low material cost and can easily be applied in larger sections. Therefore, deformation problems are often tackled with steel plates. As steel plates have no fibrous structure, bolts can be used to reduce the anchorage length. Disadvantages are the high density of steel which hampers the application, and steel plates need a special treatment against corrosion. CFRP is a lightweight flexible composite. This makes it easier to apply. It has an E-modulus comparable to steel. The tensile strength is 5 to 10 times higher than standard steel. CFRP is used for strengthening of concrete plates, because their strength can be better exploited. As the flexible sheets can easily be wrapped, CFRP is also often applied as external shear reinforcement. But, as carbon can not take shear stresses, beams have to be rounded with a radius of 3 cm. Disadvantages are the high material cost and its brittleness. Therefore, large safety factors are required.

Steel wire reinforced polymer (SWRP) is a new material that can be used as external reinforcement. It consists of thin high-strength steel fibres which are bundled into cords (see Fig. 1). These cords are woven into unidirectional sheets with a synthetic textile. SWRP combines the advantages of steel and CFRP: the composite has the same strength as CFRP but is ductile. The material cost is low and the SWRP-laminate remains quite flexible. The new composite enables the same applications as steel plates and CFRP sheets and laminates, but also new application challenges can be tackled: shear strengthening of complex shapes, wrapping of rectangular beams, and improved uses of pre-stressing.

This paper deals with the use of SWRP as external reinforcement. It consists of three parts. In the first part a feasibility study is made. Problems for the practical use of SWRP as external reinforcement are recognized. In this part, the impregnation and the flexural stiffness of SWRP are studied. In the second part, the behaviour of the bonded connection with SWRP is examined. If this behaviour can be predicted, anchorage length and transferable load can be calculated. Therefore, non-linear fracture mechanics is applied to model and describe the shear-slip behaviour of the bonded connection. Some model parameters, specific for the new material, are determined by means of direct shear tests. In the last section, the combination of bending and shear is studied. When a beam is strengthened, some extra failure modes are introduced. One of them, so called delamination, is studied in this section. The used model is tested by means of four point bending tests on beams strengthened with SWRP.

2. MATERIAL PROPERTIES

The SWRP used in the experiments of this paper is a prototype, produced by Bekaert Inc., Fig. 2. One sheet (width: 95 mm) consists of 65 steel cords. 19 filaments are twisted in a cord. The filament in the middle has a diameter of 0.25 mm, the other 18 have a diameter of 0.22 mm. By means of five tensile tests, the tensile strength and E-modulus of the SWRP are determined. The average tensile strength is 2775 N/mm², the average E-modulus is 177 600 N/mm².

To ensure a good impregnation of the cords, SWRP can be pre-impregnated. This kind of SWRP can be compared with the pre-cured CFRP laminates where impregnation is also more complete. In this research, some SWRP is pre-impregnated with an epoxy resin through vacuum impregnation followed by autoclaving at 125°C and 3 bar. Experiments are done on double layer SWRP with the epoxy resin F533 from Hexel Composites [3] with E-modulus 2900 N/mm².

3. FEASIBILITY

In practical applications, it is desirable that SWRP is glued as easily as CFRP. Such sheets can be easily wrapped because of the low flexural stiffness of the fibres. The stiffness of SWRP is investigated first, as well as the impregnation of SWRP with the adhesive.

3.1 Flexural stiffness of SWRP

The new composite enables the same applications as steel plates and CFRP but also new application domains are targeted: shear strengthening of complex forms, wrapping of rectangular beams. Since the sheets are flexible, CFRP can be easily applied, which is an important advantage in practice. When wrapping CFRP, the reinforcement sticks to the beam or column without extra auxiliary actions. Also SWRP seeks an easy application. For the proposed applications, it is important that SWRP can be wrapped and kept in place without special arrangements.

The stiffness of SWRP can be checked by calculating the cross sectional moment of inertia. Without taking into account the torsion of the filaments, the moment of inertia equals 4.05 mm^4 , Equation (1), for the type of SWRP studied in this paper.

$$I_{cord} = \sum_i (I_{filament} + A_i y_i^2) \quad (1)$$

with	A_i	section of filament i	$[\text{mm}^2]$
	y_i	distance of filament i to the neutral axis	$[\text{mm}]$

When the shape of a CFRP sheet is assumed to be a rectangular plate ($0.0167 \text{ mm} \times 95 \text{ mm}$), the moment of inertia is 0.037 mm^4 . This means that the studied type of SWRP is more than 100 times stiffer than CFRP. A decrease in stiffness can be reached if less filaments belong to a cord, or if the filaments are used single, or if other types of SWRP are used.

3.2 Impregnation

It is important that the external reinforcement can be glued, without causing a weak link in the connection. As the reinforcement is often applied above the head, viscous adhesive is used. When using this kind of adhesive, it has to be checked that all steel fibres are surrounded by the adhesive. If not, the glue is the weakest link in the connection and can cause premature failure.

The impregnation of SWRP is tested by means of six pull-off tests. Several pieces of SWRP are glued on concrete with Epicol U [4], a viscous adhesive. It is necessary that the external reinforcement is pushed into the glue, which is not convenient in practice. Therefore, new adhesives have to be developed. Pull-off test were carried out on the SWRP-laminates. On the SWRP, a cylindrical element is glued. After hardening of the adhesive, a cylindrical saw cut is made to define the failure area. Afterwards, the cylindrical element is pulled off. In Fig. 3, test samples are presented after the pull-off test. The impregnation of the cords is sufficient. All test samples have failed in the concrete, not in the adhesive or in the connection between cylinder and SWRP or between SWRP and concrete. But in the laboratory, the work is more accurately done than in practice. Therefore, it seems that enhanced impregnation is necessary. This is possible by developing new adhesives or with pre-impregnated laminates. These

laminates have a very good impregnation which does not depend on the circumstances of the site.

4. SHEAR BEHAVIOUR

When using SWRP as external reinforcement, the required anchorage length and transferable force must be known. Therefore, non linear fracture mechanics are applied to a model which describes the shear-slip behaviour of the bonded connection. At the Reyntjens laboratory of the KULeuven, model parameters are determined in a test program by means of direct shear tests.

4.1 Pure shear model

Using the equilibrium of forces, Volkersen [5] derived the following differential equation which describes the shear stresses as function of the slip of the external reinforcement:

$$\frac{d^2 s_l(x)}{dx^2} - \frac{1 + m_l \gamma_l}{E_l h_l} \tau_l(x) = 0 \quad (2)$$

in which $m_l = \frac{E_l}{E_c}$ (3)

$$\gamma_l = \frac{A_l}{A_c} \quad (4)$$

and	$s_l(x)$	slip of the external reinforcement at x	[mm]
	$\tau_l(x)$	shear stresses in the adhesive at x	[N/mm ²]
	E_l	E-modulus of the external reinforcement	[N/mm ²]
	E_c	E-modulus of the concrete	[N/mm ²]
	h_l	thickness of the external reinforcement	[mm]
	A_l	section of the external reinforcement	[mm ²]
	A_c	concrete section	[mm ²]

The best results are given by the assumption of a bilinear shear-slip relationship, Fig. 4, as shown in [6; 7]. Initially, the shear stress increases, until the maximum shear stress τ_{lm} is reached. Afterwards, concrete cracks appear in the concrete and consequently the shear stress decreases. When the ultimate slip s_{l0} is reached, no forces are transferred anymore and the connection fails. With this assumption, the solution of Equation (3) becomes:

$$s_l(x) = A \sinh(\omega x) + B \cosh(\omega x) \quad (5)$$

with: $\omega^2 = \frac{\tau_{lm}}{s_{lm}} \frac{1 + m_l \gamma_l}{E_l h_l}$ (6)

Three model parameters τ_{lm} , s_{lm} , s_{l0} are introduced in the bilinear shear-slip relationship. The shear peak stress τ_{lm} depends only on the strength properties of the concrete because failure will occur in the concrete. Applying a linear Mohr-Coulomb failure criterion [6],

748 Figeys et al.

Equation (7) can be derived from the Mohr's circle for pure shear and a tangential intrinsic curve [1].

$$\tau_{lm} = \frac{f_{ctm} f_{cm}}{f_{ctm} + f_{cm}} \quad (7)$$

with:

f_{cm}	compressive strength of concrete	[N/mm ²]
f_{ctm}	tensile strength of concrete	[N/mm ²]

However, additional parameters must be introduced to account for the relationship between the lab test and the reality, Equation (8).

$$\tau_{lm} = k_{b1} k_{b2} k_c \frac{f_{ctm} f_{cm}}{f_{ctm} + f_{cm}} \quad (8)$$

k_c is the concrete influence factor, varying between 0,65 and 1. k_c is 1 in case of good workmanship, reducing to 0.65 [1] in case of bad workmanship. k_{b1} describes the size effect for brittle materials and is given by Equation (9) [7]. The mechanical strength increases when the test sample becomes smaller.

$$k_{b1} = \sqrt{\frac{k}{1 + \frac{b_l (k-1)}{h_{ref}}}} \quad (9)$$

where b_l is the width of the external reinforcement and h_{ref} is an empirical factor. h_{ref} is the depth of the concrete that is influenced by the shear stresses in the adhesive. Holzenkämpfer [7] proposed a value of h_{ref} of 2.5 – 3 times the size of the biggest gravel stones. k is an empirical factor which takes into consideration the multi-axial stress situation. This parameter has to be determined from experiments. k_{b2} introduces a second width effect: it accounts the spreading out of the forces in the concrete, Fig. 5.

$$k_{b2} = \sqrt{2 - \frac{b_l}{b_c}} \quad (10)$$

in which b_c is the width of the concrete.

The second model parameter s_{lm} is the value of the slip at peak shear stress. The slip is determined as the sum of the slip in the different layers: the concrete (height h_{ref}), the adhesive and the external reinforcement:

$$s_{lm} = \sum_i \frac{h_i}{G_i} \tau_i = \tau_{lm} \left(2,4 \frac{h_{ref}}{E_c} + 2,5 \frac{h_g}{E_g} + 2 \cdot (1 + \nu_l) \frac{h_l}{E_l} \right) \quad (11)$$

with: h_l	thickness of the external reinforcement	[mm]
h_g	thickness of the adhesive layer	[mm]

$$G_i = \frac{E_i}{2(1 + \nu)} \quad \text{shear modulus of the } i^{\text{th}} \text{ layer} \quad [\text{N/mm}^2]$$

ν Poisson's ratio; [-]
concrete: $\nu_c = 0,2$; adhesive : $\nu_g = 0,25$; steel wire : $\nu = 0,3$

As s_{lm} depends on τ_{lm} , it also depends on the parameters k_{b1} , k_{b2} , k_c .

The last model parameter is the slip s_{l0} at which no more forces can be transferred. Therefore, a new parameter is introduced: the fracture energy G_f . This fracture energy is the energy per unit area, needed to bring a connection into complete failure. It is given by the area under the shear-slip curve, Fig. 4. In Equation (12) gives the fracture energy for a bilinear shear-slip relationship.

$$G_f = \int_0^{\infty} \tau(s_l) ds_l = \frac{\tau_{lm} s_{l0}}{2} \quad (12)$$

If the fracture energy is known, the slip s_{l0} can easily be calculated. To determine the fracture energy, following expression is proposed by Holzenkämpfer [6]:

$$G_f = k_{b1}^2 k_{b2}^2 k_c^2 C_f f_{ctm} \quad (13)$$

G_f depends on the tensile strength of the concrete. Again, the parameters k_{b1} , k_{b2} , k_c are included. A new empirical factor is introduced. C_f is a parameter fits the experiments to the model.

When the three model parameters are known, the differential equation of Volkersen can be solved. The shear stresses can be calculated at every location as a function of the external loading. Also the anchorage length and the corresponding maximum transferable load can be derived [1].

4.2 Experiments

Eight direct shear tests were executed at the Reyntjens laboratory. On four of them single SWRP is tested. Pre-impregnated double layer SWRP (marked with I) are used in the four others. The test set-up is shown in Fig. 6.

Two concrete prisms are bonded together with SWRP on two opposite sides which are grit blasted. Between the two prisms, there is a gap of 18 mm. Bonding length is 150 mm or 200 mm. On the other sides, steel plates are glued. They transfer the load from the testing machine to the test samples. Commercially available adhesive Epicol U [4] is used. This adhesive is a glue paste, its E-modulus equals 7000 MPa. After hardening, a saw-cut is made alongside the SWRP, to prohibit spreading out of forces. Therefore, k_{b2} equals 1. Since the test specimens are carefully prepared under laboratory conditions, k_c is also 1.

750 Figeys et al.

The test is deformation controlled. The change of the gap between the two concrete blocks is monitored by means of two Linear Voltage Differential Transformers (LVDT) at two opposite sides of the block, Fig. 6b. The gap increases at a constant mean rate of 0,001 mm/s. By comparing the two individual signals, one can check whether or not the tensile force acts centrally. Test 150a was oblique and is not taken in consideration.

In all test specimens, failure was due to failure of concrete. This means that the concrete is the weakest link in the connection. Test specimen I150a after failure is shown in Fig. 7.

Brosens [1] determined empirically the values of the parameters for CFRP: $k = 1,47$ mm and $C_f = 0,40$. With these parameters, a first estimation of the transferable load can be made, table 1. The model parameters are calculated with the data from table 1.

In Fig. 8, the measured tensile force and slip are compared to the model using the CFRP model parameters. In the test with single SWRP a small deviation is observed. At the end of the test, the measured curve diverges more from the model and failure took place later than predicted. The deviation on the force is about 12% and the test results are always underestimated. The SWRP seems to behave stronger and stiffer compared to elements strengthened with CFRP. The model parameters for CFRP predict the results relatively good, but are a rather conservative approach. The test results on pre-impregnated double layer SWRP are presented in Fig. 8 b. Smaller slip is measured, compared to the elements strengthened with single SWRP because of the higher amount of reinforcement. The measured curves diverge more from the CFRP-model (average deviation for the transferred forces is +20%).

In [8] a sensitivity analysis on the transferable forces is performed. Based on this analysis, it is concluded that a deviation on the material characteristics can not explain a deviation of 12% and 20% from the model. Also the sensitivity of the model parameters h_{ref} , k , C_f is examined. Changes on h_{ref} cause only small changes in the transferable forces. Parameter C_f is a factor, needed to calculate the fracture energy. It has almost no effect at small bonding lengths. The influence of C_f is only observed for long bonding length, especially longer than the theoretical anchorage length. Anchorage length can be calculated as explained in [1] : with the CFRP parameters it becomes 285 mm for the single SWRP and 399 mm for pre-impregnated SWRP with 2 layers. Finally, the parameter k takes into consideration the multi-axial stress situation. When changing this parameter, it has an influence on all bonding lengths.

All test results were systematically underestimated. The predictions of the test results on single SWRP are rather well, but in a conservative manner. The pre-impregnated SWRP laminates have a bigger deviation, so that adapted model parameters had to be proposed. The tests were made on test specimens with a small bonding length. As concluded in the sensitivity analysis, only the parameter k can be varied. Figeys proposed to decrease parameter k [8] : for single SWRP, k can be taken 1.2 mm. For pre-impregnated double SWRP, calculations with $k = 1.0$ mm give improved results. In table 2, the transferable force, calculated with the CFRP-model (F_{CFRP}) and with the adapted model parameters

for SWRP (F_{SWRP}), are compared. To evaluate the parameter C_f , additional experiments are needed for confirmation, especially tests with a longer bonding length.

5. BENDING

When a beam is strengthened, the required section is calculated from the equilibrium of internal forces. A sufficient bonding length can be provided to ensure that the forces can be introduced. However, the beam can fail in a different failure mode [9]:

- debonding of the external reinforcement,
- delamination,
- plate end shear failure,
- peeling-off of laminates at intermediate locations...

In this section the delamination is investigated for applications with SWRP.

5.1 Delamination

This failure occurs when the beam end remains unstrengthened, e. g. when the support rests on a column. At the beginning of the reinforcement, stress concentrations cause the external reinforcement to peel off. Three stresses act at the plate end: τ_l, s_b, s_n , see Fig. 9. Additional interfacial shear stresses are developed on top of the Jourawski shear stresses. Also, the plate experiences a normal stress, s_n , which peels the laminate away from the beam. Malek, Sadaatmanesh and Ehsani [10] derived the Equations (14), (15) and (16) to describe these stresses. These are derived from the equilibrium of forces, Fig. 9, assuming linear elastic and isotropic materials, perfect bond between plate and concrete, a linear strain distribution through the full depth of the section, and no interaction between shear strains and normal strains.

$$\tau_l(x) = \frac{d\sigma_l(x)}{dx} h_l \quad (14)$$

$$\frac{d^2\sigma_l(x)}{dx^2} - \frac{G_g}{h_g} \frac{1}{h_l E_l} \sigma_l(x) = - \frac{G_g}{h_g} \frac{1}{h_l E_l} \frac{E_l}{E_c} \sigma_c(x) \quad (15)$$

$$\frac{d^4\sigma_n(x)}{dx^4} + 4\beta^4 \sigma_n(x) = \frac{K_n}{E_c I_c} q(x) \quad (16)$$

in which

$\sigma_l(x)$	normal stress in the external reinforcement	[N/mm ²]
$\sigma_c(x)$	normal stress at the bottom of the concrete section	[N/mm ²]
$\tau_l(x)$	shear stresses in the external reinforcement	[N/mm ²]
$\sigma_n(x)$	normal stresses acting between the concrete and plate	[N/mm ²]
E_l	E-modulus of the external reinforcement	[N/mm ²]
E_c	E-modulus of the concrete	[N/mm ²]
E_g	E-modulus of the adhesive	[N/mm ²]
I_l	inertial moment of the external reinforcement	[mm ⁴]

752 Figeys et al.

I_c	inertial moment of the concrete	[mm ⁴]
h_l	thickness of the external reinforcement	[mm]
h_g	thickness of the adhesive	[mm]
G_g	shear modulus of the adhesive	[N/mm ²]
$q(x)$	distributed load on the concrete beam	[N/mm]

$$\beta = \sqrt[4]{\frac{K_n b_l}{4E_l I_l}} \quad [1/\text{mm}] \quad (17)$$

$$K_n = \frac{E_g}{h_g} \quad [\text{N}/\text{mm}^3] \quad (18)$$

These equations are solved at the plate end [10]. The stresses are given by eq. (21), (22) and (23), given an internal bending moment M (Equation (19)) and a shear force V (Equation (20)), Fig. 10:

$$M(x_0) = a_1 x_0^2 + a_2 x_0 + a_3 \quad (19)$$

$$V(x_0) = \frac{dM(x_0)}{dx_0} = 2a_1 x_0 + a_2 \quad (20)$$

The stresses are:

$$\sigma_l(x) = b_3 [\sinh(ax) - \cosh(ax)] + b_1 x^2 + b_2 x + b_3 \quad (21)$$

$$\tau_l(x) = b_3 h_l \omega [\sinh(ax) - \cosh(ax)] + h_l [2b_1 x + b_2] \quad (22)$$

$$\sigma_n(x) = \frac{K_n M_0}{2\beta^2 E_c I_c} e^{-\beta x} [\cos(\beta x) - \sin(\beta x)] + \frac{q(x) E_l I_l}{b_l E_c I_c} \quad (23)$$

in which

$$\omega^2 = \frac{G_g}{h_g} \frac{1}{E_l h_l} \quad (24)$$

$$b_1 = m_l \frac{y_c}{I_{tr}} a_1 \quad (25)$$

$$b_2 = m_l \frac{y_c}{I_{tr}} (2a_1 l_0 + a_2) \quad (26)$$

$$b_3 = m_l \frac{y_c}{I_{tr}} (a_1 l_0^2 + a_2 l_0 + a_3) + \frac{2b_1}{\omega^2} \quad (27)$$

$$M_0 = a_1 l_0^2 + a_2 l_0 + a_3$$

$\frac{l_0}{y_c}$ unplated length, Fig. 10

$\frac{l_0}{y_c}$ distance between the centre of the transformed section and the bottom of the beam [mm]

I_{tr} inertial moment of the beam [mm⁴]

One could derive that a peak shear stress (τ_{max}) and a peak normal peeling stress (σ_{max}) occur at the laminate end. Stresses are higher when the unplated length l_0 increases. If these two stresses make a critical combination, delamination will take place. A possible failure criterion is the Mohr-Coulomb criterion. The Mohr Coulomb line is given as Equation (28)[1]. From this value, the maximum load of the beam at delamination can be derived.

$$\tau = \frac{1}{2} \sqrt{f_{cm} f_{ctm}} \left[1 + \left(\frac{f_{cm}}{f_{ctm}} - 1 \right) \frac{\sigma}{f_{cm}} \right] \quad (28)$$

σ	normal stress in an infinitesimal part of the beam	[N/mm ²]
τ	shear stress in an infinitesimal part of the beam	[N/mm ²]
f_{cm}	mean compressive strength of concrete	[N/mm ²]
f_{ctm}	mean tensile strength of concrete	[N/mm ²]

5.2 Experiments

Five beams are examined in a four point bending test. The test setup is given in Fig. 11. The span of the beam is 1500mm. The cross section of the beam is 225mm by 125mm. The beam has a length of 1700mm. Internal reinforcement (BE 500) is provided: 3 \varnothing 8mm as tensile reinforcement, 2 \varnothing 6mm as compressive reinforcement and stirrups of \varnothing 6mm every 100mm. Concrete cover is 20mm. One beam remains unstrengthened and acts as a reference. Three beams are strengthened with one layer of SWRP ($A_l = 47,67\text{mm}^2$), the last beam is strengthened with two layers SWRP. The beams have an unplated length l_0 of 100mm or 250mm. The test specimens are listed in table 3.

The beams were tested in a load controlled testing device. The load increases with steps of 5 kN (rate: 5 kN/minute). After each step the mid span deflection is measured. At both sides of the beam demec strain gauges are applied, Fig. 12, so that strain can be followed during the test. Also, the crack pattern is recorded. The reference beam failed by yielding of the internal steel. This occurs at a load of 53 kN. All strengthened beams fail through delamination, e.g. beam 1L100b in Fig. 13. All test results are given in table 3.

5.3 Model versus experiments

A beam can fail through concrete crushing or yielding of the internal reinforcement. The load at which this kind of failure occurs can be easily calculated from the equilibrium of forces. In all cases, the internal tensile reinforcement yields first. This happens at a load of 57 kN for the unstrengthened beam, 87 kN for beams strengthened with one layer SWRP and 119 kN for the beam strengthened with two layers, table 4. These loads have to be reduced because of delamination. E.g. a beam strengthened with one layer SWRP and an unstrengthened length of 100mm will fail at a load of 77 kN. The delamination loads are listed in table 4. Remarkable is the small load, 34 kN, when the unplated length becomes large, 250 mm. This means that the beam will act as an unstrengthened beam for loads higher than 34 kN. The beam should fail through yielding of the internal reinforcement at a load of 57 kN.

754 Figeys et al.

The maximum loads of the beams 1L100a, 2L100 and the reference beam, are predicted well, with an error of respectively 4%, 4% and 7%. Beam 1L100b has a larger deviation (17%) but this remains within acceptable limits.

Beam 1L250 fails in a different way than predicted. Theoretically, the beam should fail as an unstrengthened beam because of yielding of the internal reinforcement at a load of 57kN. However, the experimental maximum load is 70kN at delamination. An unplated length of 250 mm is rather large with a shear span of 500 mm. This means that the external reinforcement starts at the middle of the span between the support and the point of application of the load. In practice, this is unusual. Possibly, this is caused by the interaction between shear, bending and spreading out of the load under the application point.

It can be concluded that the described model predicts the maximum load quite well, for reduced unplated lengths.

6. CONCLUSION

SWRP is a new material that can combine the advantages of steel plates and CFRP. It combines a relatively low material cost with a high strength and a flexible shape. For some applications (wrapping), it is necessary that SWRP has a low flexural stiffness. Therefore, it is necessary to reduce the stiffness of SWRP. Hence, new types of SWRP are required. Using SWRP as external reinforcement, the application with viscous adhesive is difficult. The impregnation is sufficient if accurately applied. The development of a new adhesive is necessary to improve impregnation. Also, pre-impregnated laminates are an interesting option.

In this paper non-linear fracture mechanics is applied to model and describe the shear-slip behaviour of the bonded connection. Experiments are presented which demonstrate that the new material behaves stronger and stiffer than elements strengthened with CFRP. Adapted material dependent parameters for SWRP for design purposes are proposed. Further experiments will be performed to confirm the general applicability of these model parameters.

When a beam is strengthened, additional failure modes have to be considered. One of them is delamination. By means of four point bending tests, it is verified that the model needs no adaptation when using SWRP. Experiments show that the model well predicts the maximum load at reduced unplated lengths.

7. ACKNOWLEDGMENT

The authors would like to thank the Flemish Institute for Promotion of Scientific and Technological Research in the Industry (IWT – Vlaams Instituut voor de Bevordering van Wetenschappelijk-Technologisch Onderzoek in de Industrie) for their financial support and to Bekaert N.V. for the materials and the support.

8. REFERENCES

- [1] Brosens, K., *Anchorage of externally bonded steel plates and CFRP laminates for strengthening of concrete elements*, doctoral thesis, Katholieke Universiteit Leuven, 2001.
- [2] Matthijs, S., *Structural Behaviour and Design of Concrete Members Strengthened with Externally bonded FRP Reinforcement*, doctoral thesis, Universiteit Gent, 2000.
- [3] Hexcel Composites, *technical data sheet F185*, 2000.
- [4] Resiplast, *Product catalogus betonherstelling*, 2003, Wommelgem.
- [5] Volkersen, O., 1938, *Die Nietkraftverteilung in zugbeanspruchten Nietverbindungen mit konstanten Laschenquerschnitten*, Luftfahrtforschung, 15, pg. 41-47.
- [6] Ranisch, E.H., *Zur Trägfähigkeit von Verklebungen zwischen Baustahl und Beton-Geklebte Bewehrung*, Heft 54, T.U. Braunschweig, 1982.
- [7] Holzenkämpfer, P., *Ingenieurmodelle des Verbunds geklebter Bewehrung für Betonbauteile*, doctoraatsverhandeling, Heft 108, IBMB, Braunschweig, pg 5-86, 1994.
- [8] Figeys, W., *Strengthening of reinforced concrete structures with bandweave (in Dutch: Versterking van gewapend beton met bandweefsel)*, Master of Science thesis, Katholieke Universiteit Leuven, 2004.
- [9] Teng, J.G.; Chen, J.F., *FRP strengthened RC structures*, John Wiley & Sons, Weinheim, 2001.
- [10] Malek, A., Sadaatmanesh; H., Ehsani, R., *Prediction of Failure Load of R/C Beams strengthened with FRP Plate Due to Stress Concentration at the Plate End*, ACI structural Journal, vol. 95, nr 2, 1998, pg 142-152.

Table 1– Prediction of transferable load with the CFRP model parameters, (F_{CFRP})

Type*	f_{ctm} (N/mm ²)	f_{cm} (N/mm ²)	h_g (mm) (epoxy adhesive)	E_g (N/mm ²)	h_{g2} (mm) (epoxy resin)	E_{g2} (N/mm ²)
1	2,65	35,0	0,98	7000	-	-
2	2,65	35,0	1,39	7000	0,65	2900
Type*	Bonding length (mm)	G_r (N/mm)	τ_{lm} (N/mm ²)	s_{lm} (mm)	s_{l0} (mm)	F_{CFRP} (kN)
1	150	0,736	2,06	0,0067	0,7134	25,9
	200	0,736	2,06	0,0067	0,7134	31,0
2	150	0,736	2,06	0,0084	0,7134	27,7
	200	0,736	2,06	0,0084	0,7134	35,0

* 1: 1 layer, 2: Pre-impregnated + 2 layers

Table 2 – Comparison between CFRP-model and adapted model

Test	Bonding length (mm)	Type *	F_{exp} (kN)	F_{CFRP} (kN)	$F_{exp}/$ F_{CFRP} (-)	F_{SWRP} (kN)	$F_{exp}/$ F_{SWRP} (-)
150 b	150	1	29,5	25,9	1,14	28,1	1,05
200a	200	1	34,4	31,0	1,10	33,6	1,02
200b	200	1	35,1	31,0	1,13	33,6	1,04
I 150 a	150	2	33,4	27,7	1,21	33,2	1,01
I 150 b	150	2	35,1	27,7	1,27	33,2	1,06
I 200 a	200	2	39,5	35,0	1,13	41,9	0,94
I 200 b	200	2	41,7	35,0	1,19	41,9	1,00

* 1: 1 layer, 2: Pre-impregnated + 2 layers

Table 3 – Results of the four point bending test.

Beam	Layers; l_θ	P_{exp} [kN]	Max. midspan deflection [mm]	failure
reference	-	53	5,02	Yielding internal reinforcement
1L250	One layer; 250 mm	70	4,77	Delamination
1L100a	One layer; 100 mm	80	6,51	Delamination
1L100b	One layer; 100 mm	90	6,96	Delamination
2L100	Two layers; 100 mm	75	3,44	Delamination

Table 4 – Calculated loads.

	Reference	One layer	One layer	Two layers
I_0 [mm ²]	-	250	100	100
τ_{imax} [P /mm ²]	-	$8.80 \cdot 10^{-5}$	$3.85 \cdot 10^{-5}$	$4.05 \cdot 10^{-5}$
σ_{nmax} [P /mm ²]	-	$1.09 \cdot 10^{-6}$	$0.44 \cdot 10^{-6}$	$1.20 \cdot 10^{-6}$
$P_{delamination}$ [kN]	-	34	77	72
$P_{bending}$ [kN]	57	87	87	119

Table 5 – Model versus experiments.

Beam	P_{theo} [kN]	Theoretical failure mode	P_{exp} [kN]	Experimental failure mode	P_{exp}/P_{theo} [-]
reference	57	Yielding internal reinforcement	53	Yielding internal reinforcement	0,93
1L250	57 (34)	Yielding internal reinforcement	70	Delamination	1,23 (2,06)
1L100a	77	Delamination	80	Delamination	1,04
1L100b	77	Delamination	90	Delamination	1,17
2L100	72	Delamination	75	Delamination	1,04

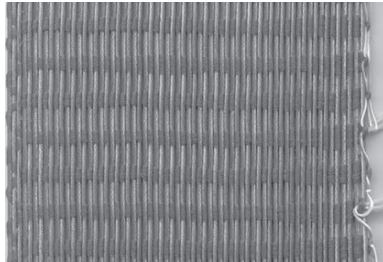


Figure 1 – SWRP, top view.

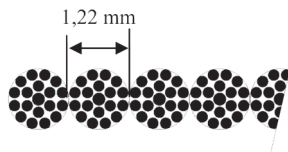


Figure 2 – SWRP, type studied in this paper, 65x [1x 0.25mm + 18x 0.22mm].

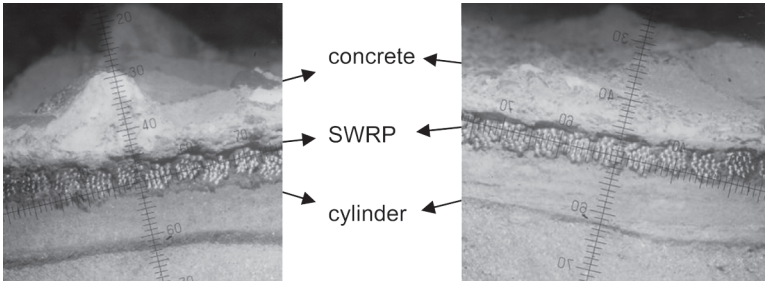


Figure 3 – SWRP, section after pull-off test.

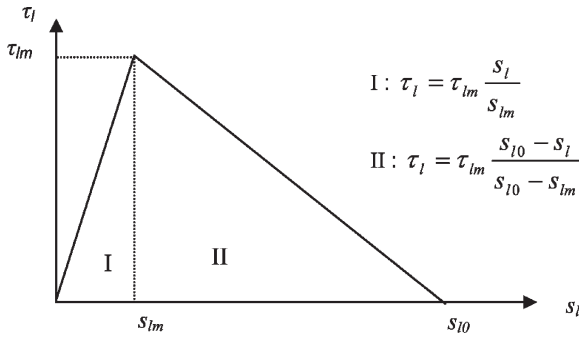


Figure 4 – Bilinear t_l - s_l relationship.

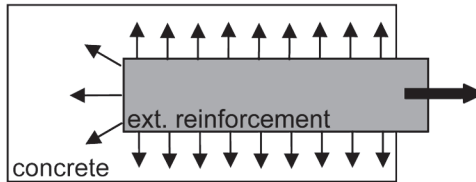


Figure 5 – Spreading out of forces in the concrete.

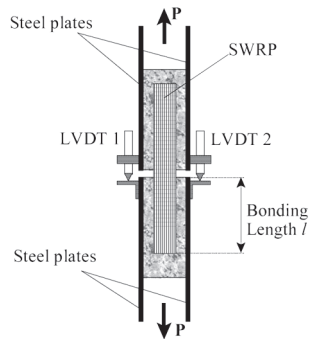


Figure 6 – a. Scheme of shear test [1]; b. photograph of test set sample.



Figure 7 – Test I150a after failure.

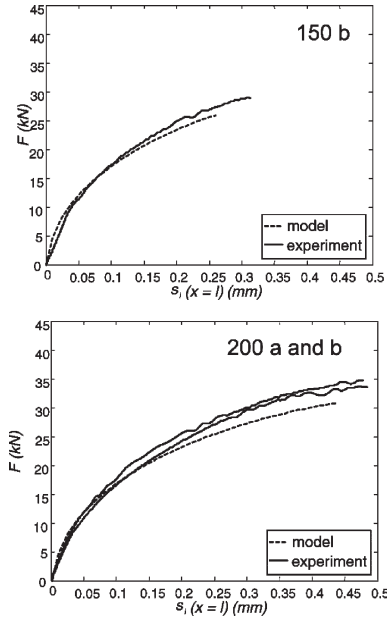


Figure 8 a – Comparison between experiment and model. Parameters single SWRP: $h_{ref} = 40$ mm, $k = 1.47$ mm, $C_f = 0.40$, $\tau_{lm} = 2.06$ N/mm², $s_{lm} = 0.0067$ mm, $s_{lo} = 0.7134$ mm.

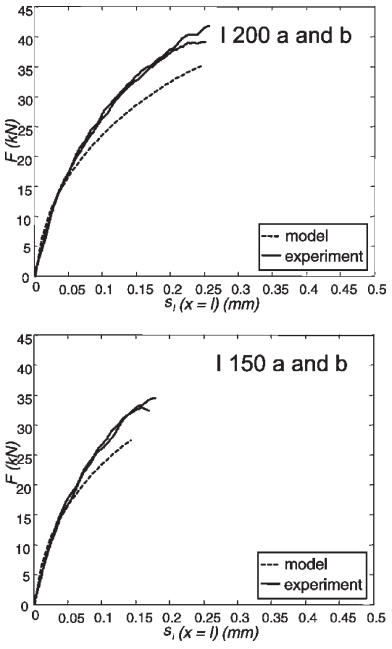


Figure 8 b – Comparison between experiment and model. Parameters pre-impregnated double SWRP: $h_{ref} = 40$ mm, $k = 1.47$ mm, $C_f = 0.40$; $\tau_{lm} = 2.06$ N/mm², $s_{lm} = 0.0087$ mm, $s_{lo} = 0.7134$ mm.

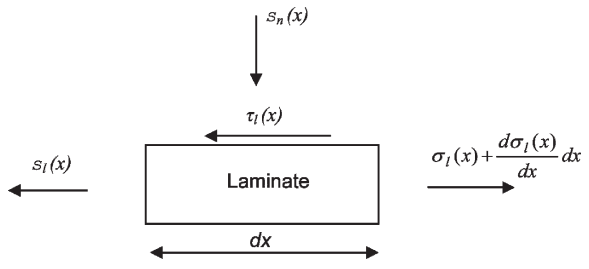


Figure 9 – Stress acting on an external laminate.



Figure 10 – Strengthened concrete beam.

762 Figeys et al.

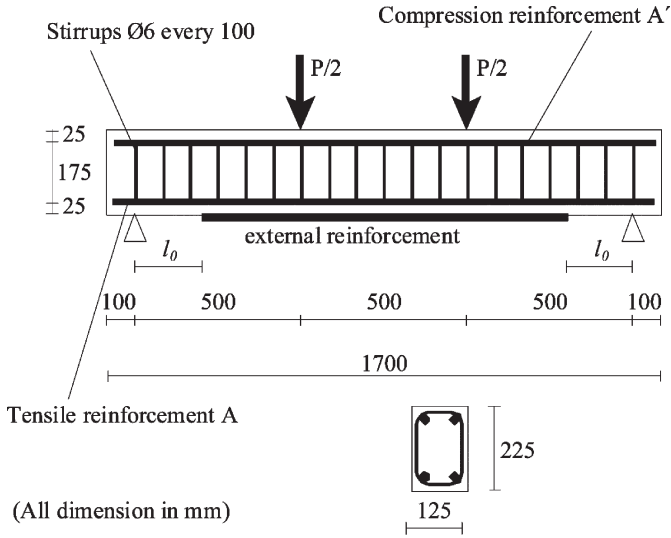


Figure 11 – Test set up four point bending test.

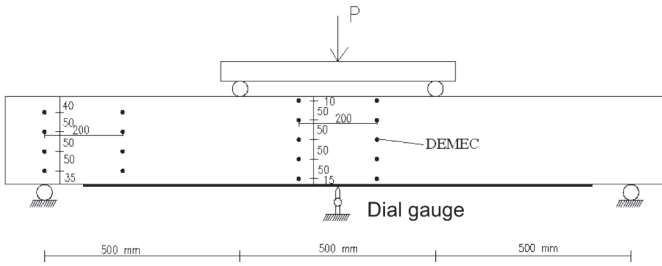


Figure 12 – Position of Demec strain gauges.



Figure 13 – Beam 1L100b, after failure.